Pergamon

Tetrahedron 56 (2000) 6951–6956

TETRAHEDRON

'Ship-in-a-Bottle' Synthesis and Photochromism of Spiropyrans Encapsulated within Zeolite Y Supercages

Isabel Casades,[a] Steven Constantine,[b] David Cardin,[b] Hermenegildo García,[a,*] Andrew Gilbert[b] and Francisco Márquez[a]

[a]*Instituto de Tecnología Química CSIC-UPV, Universidad Politécnica de Valencia, Apartado 22012, 46071 Valencia, Spain*
[b]*Department of Chemistry, University of Reading, Whiteknights, P.O. Box 224, Reading RG6 6AD, UK*

Received 26 December 1999; revised 26 February 2000; accepted 28 February 2000

Abstract—The ship-in-a-bottle synthesis of three spiropyrans inside the NaY supercages was carried out by the condensation of 2-methylene-1,3,3-trimethylindoline with the appropriate substituted benzaldehyde. After the reaction, spiropyrans were detected in the supernatant and the zeolites became coloured. Combustion chemical and thermogravimetric analyses confirmed the presence of organic material within the solid. UV–Vis and Raman spectroscopies are compatible with the formation of the merocyanine form of the spiropyran photochromic system. Upon visible irradiation the solids bleach, and in some cases the coloration is regained upon standing in the dark for long periods. This *abnormal* photochromic behaviour is the reverse of that observed for the spiropyran/merocyanine system in ethanol and illustrates the possibility of zeolites as media to alter the molecular properties of incorporated guests.

Introduction

Spiropyrans (**SP**) are the best studied photochromic compounds.[1–3] Their photochromism is due to the different UV–Vis spectra of the colourless, closed **SP** form and the intensely coloured, open merocyanine (**MC**) form and the fact that their interconversion is triggered by UV light (Scheme 1). Given the very different molecular properties of the spiro **SP** and the zwitterionic **MC** forms in terms of polarity and their tendency to form hydrogen bonds, the thermodynamic equilibrium between **SP** and **MC** and their interconversion rate is highly dependent upon the nature of any substituents (R) and the properties of the medium. Thus, an adequate combination that leads to convenient photochromic properties in solution requires a nitro group at the 6 position of the chromene ring, with ethanol as the solvent. It is worth noting that the parent **SP–H** (R=H) does not exhibit photochromism upon irradiation in ethanol since the corresponding **MC–H** (lacking a 6-NO_2 group) is much less stable and reverts more quickly to the colourless **SP–H**. Therefore, upon irradiation there is not a sufficiently high build-up of **MC–H** to surpass a threshold concentration. The influence of hydrogen bonding and complexation with transition metals in the **SP↔MC** interconversion, though not new, has attracted some interest in recent years.[4–6] It is known that minor variations on the substituents and their location as well as on the medium has a profound effect on the photochromic properties of the **SP/MC** system.

Incorporation of organic species inside the channels and cavities of microporous zeolites has proved to be a general methodology to gain control over both their molecular and photochemical properties.[7] The special properties of the

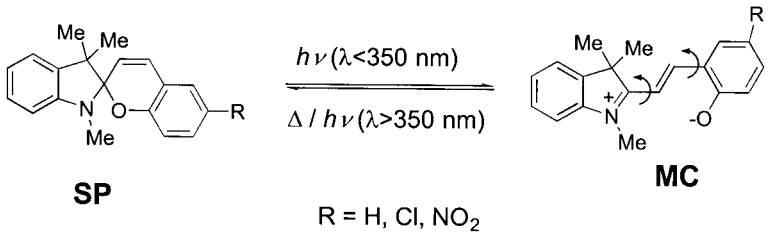

Scheme 1. Photochromic equilibrium between colourless **SP** and coloured **MC**.

Keywords: photochromism; spiropyrans; zeolite.
* Corresponding author. Tel.: +34-96-387-7807; fax: +34-96-387-7809; e-mail: hgarcia@qim.upv.es

0040–4020/00/$ - see front matter
PII: S0040-4020(00)00515-9

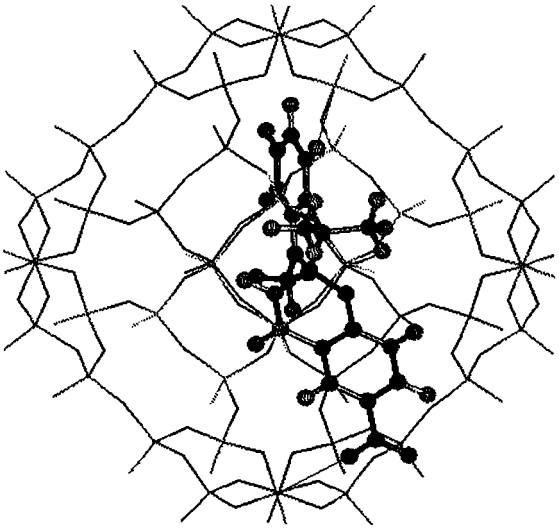

Figure 1. Molecular modeling based on semiempirical calculations showing the best docking of **SP–NO$_2$** inside the zeolite Y supercages. No significant van der Waals unfavorable overlap of guest–host atomic radii is predicted.

rigid internal voids of the zeolites in terms of polarity and the presence of charge-balancing cations, makes these crystalline aluminosilicates suitable as solid matrices to stabilise positively charged as well as zwitterionic species, increasing markedly their lifetimes compared to those measured in common organic solvents.[8,9]

In the present work, we report on the preparation and characterisation of three **SP**s inside the supercages of Y zeolite. For comparison, MCM-41 and amorphous silica–alumina has also been included in this study. In a related precedent, **SP** was adsorbed in the interlamellar region of layered clays and it was observed that the **SP↔MC** equilibrium is irreversibly shifted towards the more polar **MC**;[10–13] as a result, the supramolecular system losses the photochromic behaviour of **SP**. In other reports, the photochromism of sulfonated spiropyrans-organic modified silica nanocomposites (the position of the sulfonic group and the presence of other substituents not specified) obtained from preformed commercial spiropyrans and polymerising alkyl- or phenyl-triethoxysilane has been studied.[14,15] Herein, we have also found that the polarity of the reaction cavity provided by the zeolite host favours the coloured **MC** as the predominant form, but a certain reversible photochromism can still be observed, although the **SP↔MC** system operates in the reverse manner as that occurring in EtOH.

Results and Discussion

Due to the frozen orthogonal configuration of the indolic and chromenic moieties, **SP** is a fairly rigid molecule lacking in conformational freedom, whilst **MC** is considerably more flexible due to the permitted rotation through the simple C–C bond connecting the indolic and phenolate substructures (Scheme 1). However since pure **MC** cannot be obtained in solution, its incorporation inside Y zeolites is not feasible. On the other hand, molecular modelling at the semiempirical level predicts that even though **SP** can be accommodated inside the spherical supercavities of the Y zeolite (~1.4 nm diameter), its molecular dimensions are too large to allow its incorporation from an organic solution towards the interior of the pores since **SP** cannot cross the smaller cage windows (0.74 nm diameter). Fig. 1 shows a visualisation of the best docking of 6-NO_2 substituted **SP** (**SP–NO$_2$**) within the supercages of zeolite Y. As it can be seen there, the nitro group is partially penetrating through one of the cavity windows, indicating that this molecule occupies a little more space than that available in a single cavity. From this molecular model it can be concluded that in order to prepare **SP**-incorporating zeolite Y supercages, it is necessary to proceed using 'ship-in-a-bottle' syntheses, wherein smaller precursors that are able to diffuse freely through the pores, react inside the cage and lead, ultimately, to the formation of the target **SP**. We adopted such a methodology, stoichiometrically condensing 2-methylene-1,3,3-trimethylindoline with the appropriately substituted salicylaldehyde in CH_2Cl_2 under reflux conditions (Scheme 2). This is a general reaction that is commonly used to prepare **SP** in the absence of zeolites. Table 1 contains a

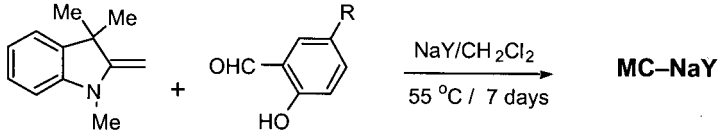

Scheme 2. 'Ship-in-a-bottle' synthesis of **SP** incorporated within zeolite Y.

Table 1. Main analytical and spectroscopic data of the samples prepared in the present work

Sample	Substituent R	Carbon content (%)	C/N Ratio	λ_{max}(nm)
MC–H/NaY	H	1.59	15.4	555 (sh 525)
MC–Cl/NaY	Cl	1.13	14.7	570 (sh 530)
MC– NO_2/NaY	NO_2	2.62	8.69	394, 530
SP–H/NaY-a[a]	H	>0.2	–	–
MC–H/SiO_2–Al_2O_3	H	>0.2	–	–
MC– NO_2/MCM-41[b]	NO_2	2.8		381, 538

[a] Prepared by adsorbing pre-formed **SP–H** from CH_2Cl_2 on NaY and subsequently submitting the solid to exhaustive solid–liquid extraction with EtOH.
[b] Prepared by adsorbing pure **SP–NO$_2$** on an all-silica MCM-41 (32 Å pore size).

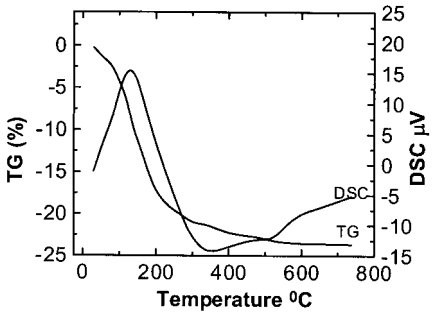

Figure 2. Thermogravimetric analysis (TG, left axis) and differential scanning calorimetry (DSC, right axis) of **MC–NO_2**/NaY.

list of the samples that have been prepared and a summary of their main analytical and spectroscopic properties.

GC analyses of the supernatant solutions after the reactions confirmed the formation of the corresponding **SP**s, in addition to lesser amounts of unreacted starting materials and indoline derived products 1,3,3-trimethyl-2-indolinone and 1,2,3,3-tetramethylindoline. In view of these results showing the formation of **SP** in the CH_2Cl_2 solutions, it is not unreasonable to expect an additional fraction of **SP** also to have been formed inside the zeolite Y supercages, and which would remain trapped in the solid after the synthesis. Thus, combustion chemical analyses (C and N) of the zeolites after exhaustive extraction with ethanol and complete removal of the solvent in vacuo revealed the presence of a significant amount of organic material (Table 1).[15] Considering that all of the organic material corresponds to **SP** the elemental analyses give a maximum occupancy estimation of one fourth of the zeolite cavities, which is a reasonable value when compared with related 'ship-in-a-bottle' syntheses.[7]

Thermogravimetric–differential scanning calorimetry studies of the spiropyran containing NaY samples give an estimation of the adsorbed organic content that also agrees with the data of chemical analyses. The thermogravimetric profiles of the samples show common features. Thus, after an initial endothermic loss of weight of approximately 20 wt% at temperatures up to 200°C, associated with the desorption of co-adsorbed water, there is a second loss of weight between 300 and 700°C (around 2 wt%) corresponding to an exothermic process, and attributed to the partial combustion/degradation of the adsorbed organic material. The fact that this second process takes place at high temperatures is commonly observed when the organic species is strongly adsorbed within the solid (Fig. 2).

However, in spite of the presence of **SP** in the supernatant solution after the synthesis indicated in Scheme 2, the spectroscopic data of the zeolite samples do not totally agree with the presence of **SP**, rather these spectra are indicative of the **MC** form being the predominant species retained in the solid. Thus, diffuse-reflectance UV–Vis spectra of the solids (Fig. 3, left) each exhibit a band in the visible region characteristic either of 2-methylene-1,3,3-trimethylindoline or the **MC** forms.[16] Comparison of the FT-Raman spectra of pure indoline specimens with those recorded for the zeolite powders after the synthesis conclusively rules out the presence of detectable amounts of indoline in the solids.[16] It was observed that co-adsorbed water plays a role in the relative intensities of the absorption bands appearing in the diffuse-reflectance UV–Vis spectra. In this regard, mild baking of the samples (110°C for 5 h) increases the absorbance of the short-wavelength maximum relative to the long-wavelength band. Comparison of the FT-Raman of pure **SP** crystals with that of the zeolites after the ship-in-a-bottle synthesis (Fig. 3, left) clearly indicates that while all the peaks corresponding to the **SP** form are present, the spectra contain other extra vibration bands. Based on the formation of **SP** in the organic phase during the synthesis and on the diffuse reflectance UV–Vis spectra, we attribute these extra vibrational peaks present in the FT-Raman spectra to the **MC** forms encapsulated within NaY in equilibrium with their spiro forms. In order to support this assignment, adsorption of pure **SP–NO_2** on an *all-silica* MCM-41 was carried out. It was observed that adsorption of **SP–NO_2** also produces the same changes in the diffuse-reflectance UV–Vis (Table 1) and Raman spectra as those observed when comparing the spectra of pure **SP–NO_2** crystals with those of the NaY powders after the ship-in-a-bottle syntheses. We attempted measurements also by FT-IR spectroscopy, but the much more intense absorption bands of the Si–O and Al–O vibrations of the zeolite lattice in the IR compared to Raman rendered these spectra much less informative. The herein proposed stabilisation of the **MC** form over the **SP** within zeolites agrees with the reported precedent on the incorporation of spiropyrans in the interlamellar region of clays.[10–13]

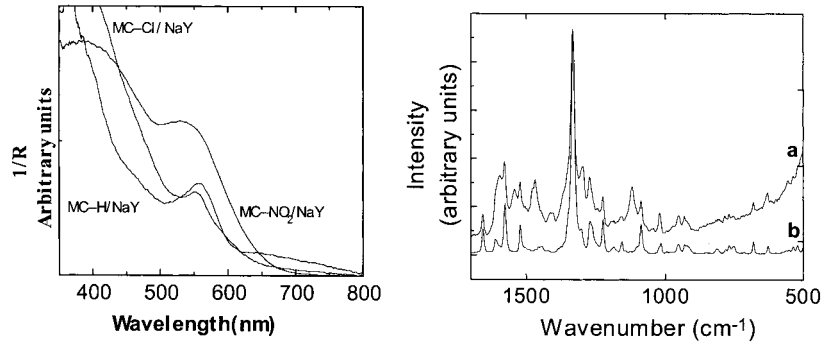

Figure 3. Left: Diffuse-reflectance UV–Vis spectra plotted as the inverse of the reflectance ($1/R$) of the NaY samples after spiropyran 'ship-in-a-bottle' syntheses and exhaustive solid–liquid extraction. Right: FT-Raman spectrum of **MC–NO_2**/NaY (a) compared to that of pure nitrospiropyran crystals (b) showing that spectrum (a) contains all the peaks of spectrum (b) plus some extra bands attributable to the **MC–NO_2** form.

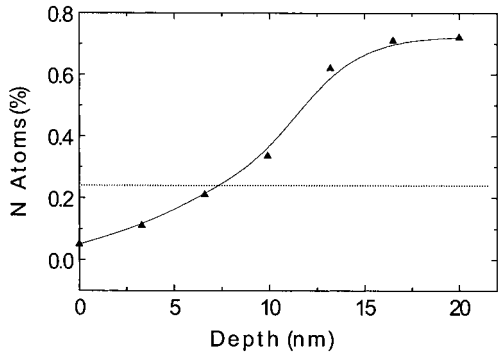

Figure 4. Percentage nitrogen atoms of the total number of atoms, measured by XPS at different depths through the zeolite particle for the **MC**–$\mathbf{NO_2}$/NaY sample. The line shows the N atom percentage calculated from the elemental analysis.

One point of concern when dealing with organic species-zeolite supramolecular systems is to be able to prove that the organic material is in fact hosted inside the micropores of the zeolite and not exclusively deposited on the external surfaces of the particles. Therefore we have performed both indirect assays and direct measurements.

Thus, the synthetic procedure depicted in Scheme 2 was carried out in the presence of amorphous silica–alumina instead of NaY: silica–alumina has a chemical composition like that of zeolites, but because it is not a microporous solid, only external surfaces are available for the guest. As expected, the organic reaction took place equally well in the presence of SiO_2–Al_2O_3 as for NaY (as assessed by the presence of **SP** in the CH_2Cl_2 supernatant). However, two notable differences were observed: (i) the predominant form in this case appears to be **SP**, based on the diffuse-reflectance UV–Vis spectrum of the solid; and (ii) essentially all of the organic material is removed by exhaustive solid–liquid extraction with ethanol (see Table 1, entry **MC**–**H**/SiO_2–Al_2O_3). The lower polarity of the external surface of silica–alumina compared to that of the zeolite interior would account for the shift in the relative stability between the **SP** and **MC** forms, whilst since all of the organic material is recoverable, the implication is that the structure of the zeolite plays a role in retaining a significant fraction of the organic material. Likewise, in another experiment, pure **SP** was adsorbed onto NaY (supposedly on its external surface) and the resulting material then submitted to solid–liquid extraction. Again, neither the diffuse-reflectance UV–Vis spectrum corresponded to that of **MC** recorded using the ship-in-a-bottle procedure nor after exhaustive extraction was any organic material left in the solid (see Table 1, entry **SP**–**H**/NaY-a and the corresponding footnote). This result suggests that the adsorption procedure leaves **SP** deposited on the less-polar external surface of the particles from where it can readily be desorbed. As predicted by molecular modelling, no penetration of the **SP** into the pores seems to have occurred.

To provide direct experimental evidence for the distribution of the organic material within the zeolite, a sample of **SP**–$\mathbf{NO_2}$ was analysed by X-ray photoelectron spectroscopy (XPS) coupled with Ar^+-ion sputtering. XPS gives a chemical analysis of the outermost exposed layers of the zeolite grains, and by combining this surface analytical technique with fast-ion bombardment (which results in partial destruction of the external layers), it is possible to map out the chemical composition from the external surface of the zeolite to several nanometers towards the interior of the particle. Fig. 4 shows the experimental percentage of nitrogen atoms against the total number of atoms monitored as a function of the depth from the exterior of the particle. These data clearly prove that the nitrogen-containing organic material is spread out through the bulk of the particle with its abundance increasing with increasing depth. Furthermore, the organic material in the external surface has a nitrogen content below the average of the whole particle obtained from the combustion chemical analyses data.

All the coloured **MC**–NaY powders undergo a significant bleaching upon visible light irradiation, the behaviour being the reverse of that observed for the corresponding **SP**s in ethanol. Thus, irradiation (λ>450 nm) produces a progressive decolouration of the solid and the course of the photochemical transformation is conveniently followed by monitoring the decrease in the intensity of the visible band (550 nm) of the samples. Once the intensity of the visible band reaches the minimum, dark storage of the solid produces over long time periods a remarkable, though incomplete recovery of the original intensity. The

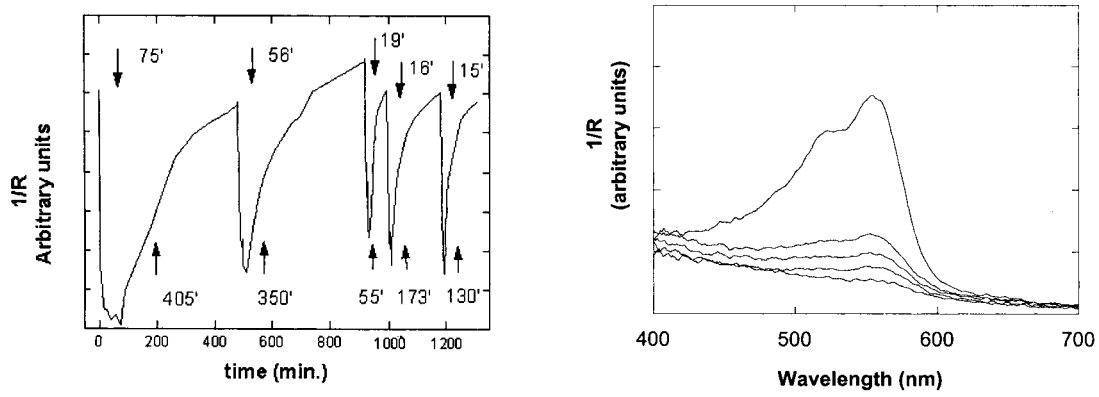

Figure 5. Left: Variation of the inverse of the reflectance (R) measured at 555 nm as a function of time during consecutive irradiation-dark storage cycles for the **MC**–**H**/NaY sample. The arrows indicate when the irradiation is on and off and the time elapsed in each cycle. Right: Diffuse reflectance spectra of the same sample at 10 min interval during irradiation.

percentage of the intensity recovery and the required time is extremely dependent upon the nature of the substituent R present in the chromenic moiety. Attempts to observe an increase in the rate of the **SP↔MC** interconversion by illuminating with UV light were unsuccessful. A precedent in solution of reverse photochromic behaviour of a series of 6-nitrospiropyrans containing two additional electron-withdrawing substituents has been reported.[17]

This cycling [(i) irradiation (λ>450 nm) in the visible with bleaching of the visible band, and (ii) recovery of the visible band in the dark] was repeated several times, with a certain fatigue of the system, in terms of a less profound decolouration, being apparent after the second cycle (Fig. 5). It is noteworthy that the photochromic response of the **MC–H/SP–H** pair (which is not observed in ethanol) is the most convenient when the compounds are incorporated within NaY. Thus, it is remarkable that under identical experimental conditions the irradiation time necessary to observe a response for the **MC–NO$_2$/SP–NO$_2$** pair is much longer. As in solution, this fact probably reflects the influence of the nitro group stabilising the **MC** form relative to the **SP** form. Given the polarity of the zeolite cages **MC–NO$_2$** becomes too stable to readily cyclise with high quantum yield to the **SP** form. The photochromic response of **MC–H**–NaY during some consecutive cycles is presented in Fig. 5.

Since the photochemical transformation of **MC** into **SP** and the subsequent thermal reversion back to **MC** upon standing on the dark takes place within minutes or hours, it is also possible to follow the course of these processes with conventional FT-Raman spectroscopy. In agreement with the variations in the diffuse-reflectance study, the FT-Raman spectra of the samples revealed a decrease in some vibrational bands of the original spectrum and the appearance of new absorptions, some of them compatible with the partial formation of **SP**. As an example, Fig. 6 shows the case of **MC–NO$_2$**/NaY, wherein the peaks increasing in intensity upon irradiation have been labelled with asterisks.

Besides characterisation by FT-Raman spectroscopy, the fact that **MC** is the stable form of the spiropyran system allows us to determine other photochemical properties. In particular, we have been able to record the emission and

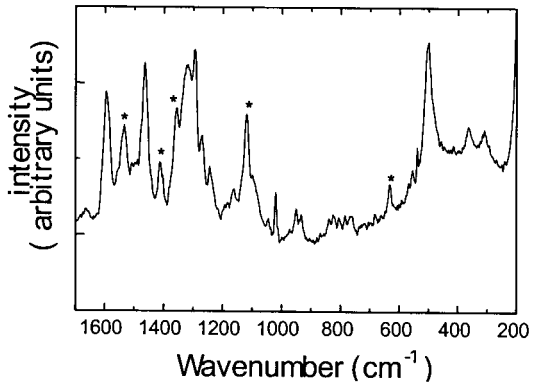

Figure 6. FT-Raman spectra of the **MC–NO$_2$**/NaY sample after irradiation with λ>450 nm. The original spectra corresponds to that shown in Fig. 3, left for the same sample and the most characteristic bands that have grown upon irradiation are marked with asterisk.

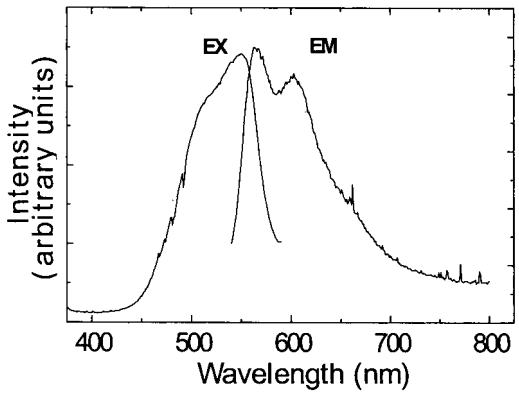

Figure 7. Emission (EM, λ_{exc} 520 nm) and excitation (EX, monitoring at 610 nm) spectra of **MC–NO$_2$**/NaY solid.

excitation spectra of the three **MC–R**/NaY samples. Thus, the excitation spectrum of the **MC** forms coincided with its UV–Vis absorption spectra and is the mirror image of the emission (Fig. 7).

In conclusion, the reaction of 2-methylene-1,3,3-trimethylindoline with substituted salicylaldehydes in the presence of dehydrated NaY leads to the formation of the spiropyrans (**SP**s) in the organic phase and the encapsulation inside the zeolite cages of some organic material that corresponds, at least in part, to the merocyanine (**MC**) form of these spiropyrans. The polarity of the zeolite pores seems to be responsible for the change in the relative stability between the **SP** and the **MC** forms that favours the latter. These **MC**-containing zeolitic materials exhibit a certain photochromic behaviour that is the reverse of that found for such organic species (**SP/MC**) when in EtOH solution, i.e. bleaching of the 550 nm band upon irradiation and the recovery of this visible band upon standing in the dark. Although further work is obviously necessary to optimise the ship-in-a-bottle synthesis, maximising the loading and improving the photochromic response of these materials probably by using more suited zeolites, the present work shows the opportunities that zeolites offer as solid hosts to incorporate light switchable molecules to prepare advanced materials with adequate optical properties.

Experimental

Combustion chemical analyses were carried out using a Fisons EA-1108 analyser. Thermogravimetry–differential scanning calorimetry studies were conducted using a Netzsch STA 409 thermobalance under air stream and kaolin as inert standard. Diffuse-reflectance UV–Vis spectra were recorded using a Cary 5G spectrophotometer adapted with a 'praying mantis' accessory for solid samples, using $BaSO_4$ as the standard. Molecular modelling was carried out at the semiempirical level using the *Insight II* package, running on a Silicon Graphics workstation. FT-IR spectra were recorded at ambient temperature using a Nicolet FT-710 spectrophotometer using sealed cells fitted with CaF_2 windows. The zeolite wafers (10 mg) were compressed at 1 Ton cm^{-2} and outgassed under 10^{-2} Pa at 100°C for 1 h. FT-Raman spectra were recorded using a Bio-Rad FT-Raman II spectrophotometer, with the

1064 μm line of a Nd:YAG laser for excitation and a liquid nitrogen-cooled Ge detector. The laser power at the sample was approximately 100 mW and the spectral resolution 4 cm^{-1}. The number of scans varied from 400 to 1000. The Raman spectra were corrected for instrumental response using a white light reference spectrum. XPS measurements were carried out at ambient temperature with a concentric hemispherical analyser operated in the constant pass energy mode (50 eV). A Mg K_α X-ray source ($h\nu$=1253.6 eV) was used. The analysis chamber was maintained at ca. 5×10^{-9} Torr during acquisition of the XPS spectra. Charging effects were calibrated by the C(1s) line at 284.6 eV. Sputtering of the samples to obtain the atomic profile of the samples was carried out inside the chamber using an Ar^+ ion gun. The response of each atom was corrected by the corresponding response factor.

Zeolite NaY (P.Q. Industries), silica–alumina (BASF, 25 wt%),2-methylene-1,3,3-trimethylindoline and the three *p*-substituted benzaldehydes (Aldrich) were commercial samples and used as received. *All*-silica MCM-41 was prepared as reported.[18] Pure specimens of the three spiropyrans were obtained by double recrystallisation of the solids, prepared by the stoichiometric condensation of 2-methylene-1,3,3-trimethylindoline (200 mg) and the corresponding benzaldehyde in ethanol (20 ml) at room temperature.

The 'ship-in-a-bottle' syntheses of the NaY-incorporated **SP**s was carried out by heating a stirred suspension of dehydrated (500°C, overnight) NaY (1 g) zeolite in an equimolar mixture of indoline (30 mg) and the corresponding benzaldehyde in CH_2Cl_2 (25 ml) under reflux conditions for seven days. At the end of the reaction, the solid was filtered and the supernatant CH_2Cl_2 analysed by GC (Hewlett–Packard chromatograph provided with a 25 m capillary column of crosslinked 5% phenylmethylsilicone) and GC–MS (Varian using the same type of capillary column as for the GC). Characterisation of the corresponding **SP** in the supernatant was carried out by comparison of the retention time and MS spectra with authentic specimens. The coloured zeolite was then submitted to exhaustive solid–liquid extraction with a micro-Soxhlet apparatus with EtOH as the solvent. Irradiation of the solid powders was carried out using an Oriel photoreactor adapted with a 420–630 nm dichroic filter (Oriel part#66219). Emission spectroscopy was recorder in a Edinburg FL-900 spectrofluorimeter using a front face attachment for solids. The samples were N_2 purged.

Acknowledgements

Financial support of the European Union (Brite BE97-4455) and the Spanish DGICYT (grant MAT97-1060-CO2) is gratefully acknowledged as it is a scholarship for I. C. from the Universidad Politécnica Valencia.

References

1. Bertelson, R. C.; Brown, G. H. Photochromism, Wiley: New York, 1971.
2. Durr, H.; Bouas-Laurent, T. H. Photochromism: Molecules and Systems, Elsevier: Amsterdam, 1990.
3. Maeda, K. *J. Synth. Org. Chem. Jpn* **1991**, *49*, 554–565.
4. Winkler, J. D.; Bowwen, C. M.; Michelet, V. *J. Am. Chem. Soc.* **1998**, *120*, 3237–3242.
5. Inouye, M.; Akamatsu, K.; Nakazumi, H. *J. Am. Chem. Soc.* **1997**, *119*, 9160–9165.
6. Suzuki, T.; Lin, F. -T.; Priyadashy, S.; Weber, S. G. *Chem. Commun.* **1998**, 22685–22686.
7. Scaiano, J. C.; García, H. *Acc. Chem. Res.* **1999**, *32*, 783–793.
8. Corma, A.; García, H. *Top. Catal.* **1998**, *6*, 127–140.
9. Cano, M. L.; Cozens, F. L.; Esteves, M. A.; Márquez, F.; García, H. *J. Org. Chem.* **1997**, *62*, 7121–7127.
10. Tomioka, H.; Itoh, T. *J. Chem. Soc., Chem. Commun.* **1991**, 532–533.
11. Takagi, K.; Kurematsu, T.; Sawaki, Y. *J. Chem. Soc., Perkin Trans 2* **1995**, 1667–1671.
12. Seki, T.; Ichimura, K. *J. Chem. Soc., Chem. Commun.* **1987**, 1187–1189.
13. Hori, T.; Tagaya, H.; Nagaoka, T.; Kadokawa, J.; Chiba, K. *Appl. Surf. Sci.* **1997**, *121*, 530–533.
14. Tagaya, H.; Nagaoka, T.; Kuwahara, T.; Karasu, M.; Kadokawa, J.; Chiba, K. *Microp. Mesop. Mater.* **1998**, *21*, 395–402.
15. In the cases of salicylaldehyde and 4-chlorosalicyladehyde, nitrogen analyses selectively traces indoline derived products including spiropyrans adsorbed in the solid.
16. Indoline is an intensely coloured compound with a band in the visible region, at 550 nm. This λ_{max} is very close to that of **MC**s. The FT-Raman sample was prepared by the adsorption of the indoline onto NaY in EtOH solution.
17. Barachevskii, V. A.; Strokach, Y. P.; Valova, T. M.; Arsenov, V. D.; Gorelik, A. M. *Zh. Nauchn. Prikl. Fotogr.* **1997**, *42*, 14–21; cf. *Chem. Abstr.* **1997**, *128*, 173979.
18. Corma, A.; Fornés, V.; García, H.; Miranda, M. A.; Primo, J.; Sabater, M. J. *J. Am. Chem. Soc.* **1994**, *116*, 9767–9768.